

Regular Article

Solute partitioning in multi-component γ/γ' Co–Ni-base superalloys with near-zero lattice misfitS. Meher^{a,*}, L.J. Carroll^a, T.M. Pollock^b, M.C. Carroll^a^a Materials Science and Engineering Department, Idaho National Laboratory, Idaho Falls, ID 83415, USA^b Materials Department, University of California Santa Barbara, Santa Barbara, CA 93106, USA

ARTICLE INFO

Article history:

Received 20 July 2015

Received in revised form 23 October 2015

Accepted 24 October 2015

Available online 21 November 2015

Keywords:

Co-base superalloys

APT

TEM

Partitioning

Lattice misfit

ABSTRACT

The addition of nickel to cobalt-base alloys enables alloys with a near zero $\gamma-\gamma'$ lattice misfit. The solute partitioning between ordered γ' precipitates and the disordered γ matrix have been investigated using atom probe tomography. The unique shift in solute partitioning in these alloys, as compared to that in simpler Co-base alloys, derives from changes in site substitution of solutes as the relative amounts of Co and Ni change, highlighting new opportunities for the development of advanced tailored alloys.

© 2015 Elsevier Ltd. All rights reserved.

The recent discovery of thermodynamically stable $L1_2$ γ' precipitates in cobalt-base (Co-base) alloys [1] provides exciting opportunities for high-refractory containing compositions with varying phase chemistries and associated lattice misfits. Extensive research efforts focusing on Co-base alloys have emerged in order to investigate and optimize their high temperature operational capability [2–13]. More recently, studies have focused on Co-base alloys containing significant additions of nickel that represent a new type of alloy, Co–Ni-base [5–10]. There are substantial advantages to additions of Ni to Co-base alloys, such as an increased γ' solvus temperature and the expansion of the γ' phase field [5,6]. Further, dramatic differences in the shearing behavior of the γ' precipitates have been reported and attributed to differences in the superlattice intrinsic stacking fault (SISF) and anti-phase boundary (APB) energies [6–8]. Since variations in these fault energies are very sensitive to the composition of the constituent phases [14], an improved understanding of the partitioning of quaternary and higher order additions is essential for controlling these energies, and ultimately the mechanical properties of these alloys.

Atom probe tomography (APT) studies have provided sub-nanometer chemical information for Ni-base superalloys [15–18] and Co-base superalloys [19–23]. The corresponding atomistic experimental studies of Co–Ni-base superalloys with approximately equal proportions of Co and Ni are limited. To date, two such studies have been reported, including one on a quaternary alloy [22] and a second on a single multi-component

Co–Ni alloy [9]. The general trend for partitioning of W in Co–Ni alloys has also been systematically investigated through microprobe analysis of coarsened γ' precipitates [5]. However, further detailed atomistic studies of multicomponent Co–Ni-base alloys are needed to gain a deeper understanding of the chemical origins of the lattice misfit, fault energies and ultimately the γ' shearing behavior.

The limited γ' phase field [1] and strong γ/γ' partitioning of W in ternary and quaternary Co-base alloys [22] make control of lattice misfit exceedingly difficult. The addition of Ni, however, provides additional design flexibility since the strong partitioning of W is tempered [5,22]. In the present study, two multicomponent polycrystalline Co–Ni-base alloys with near-zero mismatch, originally introduced in the work of Titus et al. [6] as Co–Ni–B and Co–Ni–D, have been studied using atom probe tomography (APT). The lattice misfit is near-zero based upon the spherical shape of precipitates and the absence of directional coarsening during high temperature creep deformation [6]. Fundamental information on the γ/γ' solute partitioning coefficient and the associated relative site substitution tendencies within γ' precipitates is essential for: (i) the development of $\gamma + \gamma'$ Co–Ni-base alloys with lower density and reduced γ' coarsening kinetics, and (ii) validation of the dependence of high temperature mechanical properties on γ' composition.

The bulk compositions of as-cast buttons of Co–Ni–B and Co–Ni–D (Table 1) were measured by Evans Analytical Group using inductively coupled plasma spectroscopy (ICP). The alloys were homogenized at 1215 °C for 15 h, followed by furnace cooling to room temperature at an average cooling rate of 7 °C/min. The samples were then annealed at 950 °C for 40 h and subsequently water quenched to achieve a

* Corresponding author.

E-mail address: Subhashish.meher@inl.gov (S. Meher).

Table 1

The alloy composition (in at.%) and the average composition of γ and γ' phases, estimated from APT.

Alloy	Composition	Co	Ni	Al	W	Cr	Ta	Mo	Basic composition
Co–Ni–B	Bulk	43.5	27	11	6.2	10	2.3		Co-dominant
	γ	43.2	24	8	7	17	0.8		
	γ'	36.5	34	13	7	6	3.5		
Co–Ni–D	Bulk	44	29	11.8	5.2	6	2	2	Co-dominant
	γ	47.2	25	7	5	12	0.8	3.2	
	γ'	37.5	32	12	9	4	3.5	1.7	
V208C [9]	Bulk	36.1	34.2	10.5	3	14.8	1.0		Ni-dominant
	γ	44.8	23.8	4.7	2	24.6	0.1		
	γ'	25.2	48.5	16.6	3.3	4.7	1.7		

near-equilibrium composition of the constituent γ and γ' phases. Scanning electron microscopy (SEM) studies were conducted using a Quanta 650 Field Emission Gun Scanning Electron Microscope. The γ' precipitate sizes and their associated volume fraction in each sample were obtained from analysis of SEM micrographs using IMAGE J™ software. Samples for transmission electron microscopy (TEM) were prepared by electro-polishing using a solution of 95% methanol and 5% perchloric acid, operated at -30 °C with a voltage of 18–20 V and current of 25–35 mA. TEM analysis was conducted on a FEI Tecnai F30 microscope operated at 300 kV. For atom probe tomography (APT), samples were prepared utilizing the focused ion beam (FIB) technique on a FEI Quanta 3D FEG dual-beam instrument. The APT experiments were carried out using a local electrode atom probe system (LEAP 4000 \times HR) from Cameca Instruments. All atom probe experiments were carried out in the voltage evaporation mode at a temperature of 60 K, with an evaporation rate of 0.5%. Subsequent data analysis was performed using IVAS 3.6.6 software.

Fig. 1 shows centered dark-field TEM micrographs of the two Co–Ni–base alloys with uniformly distributed mono-modal γ' precipitates with near-spherical morphology. The precipitate size distributions are similar and range from 250 to 300 nm, with a volume fraction of γ' precipitates of approximately 55%. Based on the absence of directional coarsening during high temperature creep, the near-zero γ/γ' lattice misfit of these alloys has been confirmed for both Co–Ni–B and Co–Ni–D alloys [6]. A slow cooling rate following solutioning typically results in multiple generations of γ' precipitates in highly supersaturated alloy systems [13], yet the complex interplay between the degree of supersaturation and γ' nucleation temperature at this particular cooling rate produces only a single generation of γ' precipitates in the present alloys. The degree of coalescence of precipitates in Co–Ni–D appears higher as compared to that in Co–Ni–B, possibly due to differences among lattice parameters, elastic constants or interdiffusion coefficients in the γ and γ' phases in these alloys, as described by Ardell [24].

Fig. 2(a) shows an APT reconstruction of Co–Ni–B with only Ta ions and the γ/γ' interface has been delineated by the selection of an 8 at.%

Cr iso-concentration surface (isosurface). Fig. 2(b) shows the proximity histogram (proxigram) [25] across the γ/γ' interface, created using the 8 at.% Cr isosurface, which reveals the solute partitioning in Co–Ni–B alloy. The elements Al, Ta and Ni partition strongly towards γ' precipitates, while Co and Cr partition towards the γ matrix. Of particular significance regarding the near-zero misfit goal is that W does not preferentially partition to either of these two phases. Table 1 lists the average composition of γ and γ' phases determined from APT in the present alloys. Although the strict stoichiometric division between Ni- or Co-based γ' is based upon the necessity for W at the X site of M_3X compound (γ') [11,12], for the purpose of this work, the composition of the $L1_2$ γ' phase will be defined as Co-dominant if the amount of Co in the M site is greater than the amount of Ni and Ni-dominant if the amount of Ni is greater than the amount of Co. The composition of the γ' precipitates in the investigated alloys can then be regarded as Co-dominant based on the higher amount of Co than Ni.

The partitioning coefficient ($K_{\gamma'/\gamma}$) represents the ratio of equilibrium compositions of a particular element in the γ' compared to the γ phase. Table 2 lists $K_{\gamma'/\gamma}$ for each element determined from APT, both in the present alloys and in previously reported Co–base alloys. Shinagawa et al. reported a suppression of $K_{W(\gamma'/\gamma)}$ to a value of 1.07 in a Co–Al–W base alloy with large additions of Ni with Co/Ni ratios of up to 0.65 [5]. In a multicomponent alloy, such as the Co–Ni–B, the W partition coefficient reaches a value close to 1 at a much lower relative Ni content (Co/Ni ratio = 1.6). This result is corroborated by the energetic preference of Ta and Mo for replacing W in the (Al,W) sublattice of the $Co_3(Al,W)$ compound [21,22,26], leading to a further decrease in $K_{W(\gamma'/\gamma)}$ with Co/Ni ratios greater than 1. The differing solute partitioning coefficients in these Co–Ni multicomponent alloys, as compared to Co–Al–W ternary alloys and their quaternary variants, potentially offer opportunities to develop predefined microstructural features and γ/γ' lattice misfits.

A possible enrichment of W at the γ/γ' interface, observed in multiple specimens of Co–Ni–B, is illustrated from the composition profile in Fig. 2(c). Due to the short duration of the isothermal heat treatment at 950 °C, it is difficult to conclude whether this is a kinetic effect during cooling from high temperature in which W is rejected from either the matrix or precipitate and resides at the interface, or is a result of the equilibrium segregation of W at interface necessary to reduce the interfacial energy. In APT studies of a multicomponent Ni–base superalloy, W segregation observed at {001} interfaces of cuboidal γ' precipitates has been attributed to equilibrium segregation and accommodation of strain [27]. The segregation of a large element at the interface to accommodate misfit in an alloy with similar lattice parameters of both the γ and γ' phases, such as Co–Ni–B, is unlikely. Fig. 2(d) shows a two dimensional (2D) composition contour of W ions within the APT reconstruction created using a region of interest (ROI) of $20 \times 1 \times 17$ nm and placing it across the interface for better quantitative visualization. The composition map in the x–z direction of the box more clearly shows an enrichment of W at the interface. Additional atom probe studies on

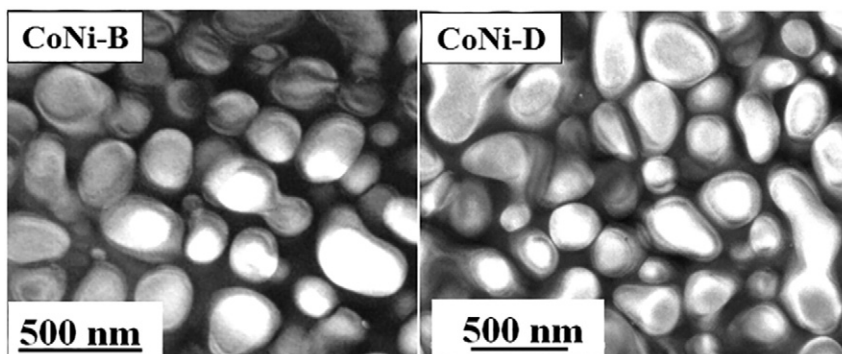


Fig. 1. Centered dark field TEM micrographs of the γ – γ' microstructures of two Co–Ni–base superalloys with near-zero lattice misfit.

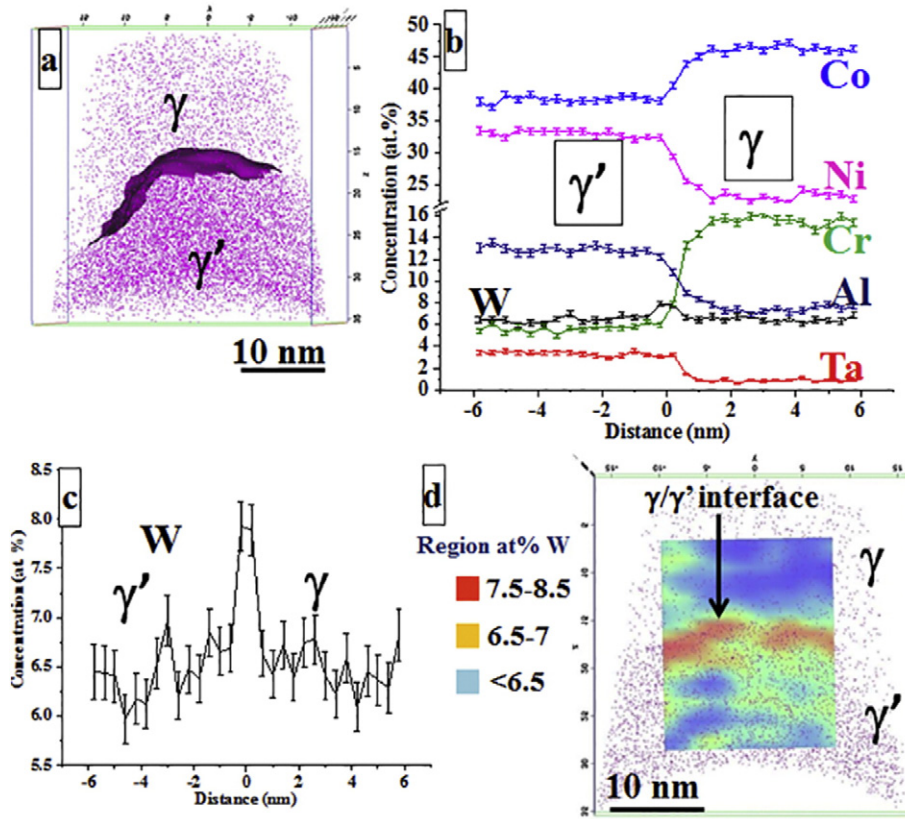


Fig. 2. (a) An APT reconstruction illustrating the partitioning of Ta ions along with a γ/γ' interface delineated by 8 at.% Cr isosurface and (b) the proximity histogram (proxigram) showing the solute partitioning across the γ/γ' interface in Co–Ni–B. (c) The magnified proxigram showing the W pile up at the interface and (d) a two-dimensional (2-D) compositional contour with respect to W ions, across the γ/γ' interfaces indicating a W pile up at the interface.

samples annealed for longer times are underway to determine the nature of this W enrichment.

Fig. 3(a) shows a proxigram, created using 8 at.% Cr isosurface, for element specific γ/γ' partitioning in the Co–Ni–D alloy. The corresponding APT reconstruction capturing both the γ and γ' phase is shown as an inset. Fig. 3(b) shows the partitioning behavior of selected elements for a better visualization. The partitioning behavior of Co, Ni, Cr, Ta, and Al are similar to those in Co–Ni–B, whereas W partitions to the γ' precipitates. The absence of a W pile up at the interface in this alloy may be attributed to the partitioning of W, maintaining a driving force for diffusion to the precipitate. The γ' phase chemistry also indicates a Co-dominant compound. In Co–Ni–D, the Mo partitioning is reversed relative to its behavior in Co-base alloys [21] exhibiting a tendency to partition to the γ matrix. The relatively large atomic radius of Mo and its preference for the γ matrix in Ni-base alloys increases the γ lattice parameter relative to that of γ' [28], the same effect can be expected for Co–Ni-base alloys. These partitioning and site substitution tendencies present new options for tailoring Co–Ni-base alloy microstructures to (1) facilitate the retention of high volume fractions of γ' precipitates with low amounts of W, not possible in ternary and quaternary Co-base

alloys, and (2) increase the solid solution strengthening component of the γ matrix with higher W content.

Previous computational studies report changes in the atomic binding energies in the basic $\text{Co}_3(\text{Al,W})$ compound through alloying [12,13] that are consistent with experimentally determined partitioning and site substitution tendencies within the γ' in less compositionally complex alloys [21,22]. For example, Ta has a strong preference for the W site in γ' precipitates in quaternary alloys [13,21] and also demonstrates similar phase partitioning behavior in the present multicomponent Co–Ni-base alloys. In contrast, Mo does not increase the binding energy to the extent of Ta and therefore exhibits a relatively weaker preference for the W site [13]. It is therefore not surprising that its weak γ' partitioning in a Co–Al–W–Mo alloy [21] is reversed in multicomponent alloys such as Co–Ni–D due to increased site substitution competition for the (W,Al) site in $\text{Co}_3(\text{Al,W})$. This evidence of reversed Mo partitioning, driven by other solutes in the γ' precipitates, provides insight into the relative influence on phase partitioning of the alloying elements in a multicomponent alloys.

When considered in combination with the recent work of Knop et al. [9] on a similar multicomponent Co–Ni-alloy, the APT results of the

Table 2

A comparison of solute partitioning coefficients (γ'/γ) of present Co–Ni-base alloys with those of ternary and quaternary Co-base alloys. The γ/γ' elemental partitioning is indicated by the magnitude of $K_{\gamma'/\gamma}$. $K_{\gamma'/\gamma} > 1$ indicates partitioning towards the γ' precipitates and $K_{\gamma'/\gamma} < 1$ indicates partitioning towards the γ matrix.

Alloys (at.%)	$K_{\text{Co}(\gamma'/\gamma)}$	$K_{\text{Ni}(\gamma'/\gamma)}$	$K_{\text{Al}(\gamma'/\gamma)}$	$K_{\text{W}(\gamma'/\gamma)}$	$K_{\text{Ta}(\gamma'/\gamma)}$	$K_{\text{Cr}(\gamma'/\gamma)}$	$K_{\text{Mo}(\gamma'/\gamma)}$
Co–7Al–7W [21]	0.83		1.6	6.2			
Co–25Ni–7Al–7W [21]	0.77	1.16	1.98	2.43			
Co–10Al–10W–2Ta [20]	0.9		1.04	2.72	5.47		
Co–10Al–10W–3Mo [20]	0.9		1.52	2.12			1.26
V208C [9]	0.56	2.0	3.5	1.7	17	0.19	
Co–Ni–B (present study)	0.77	1.57	1.62	1	4.3	0.35	
Co–Ni–D (present study)	0.79	1.28	1.7	1.8	4.3	0.33	0.66

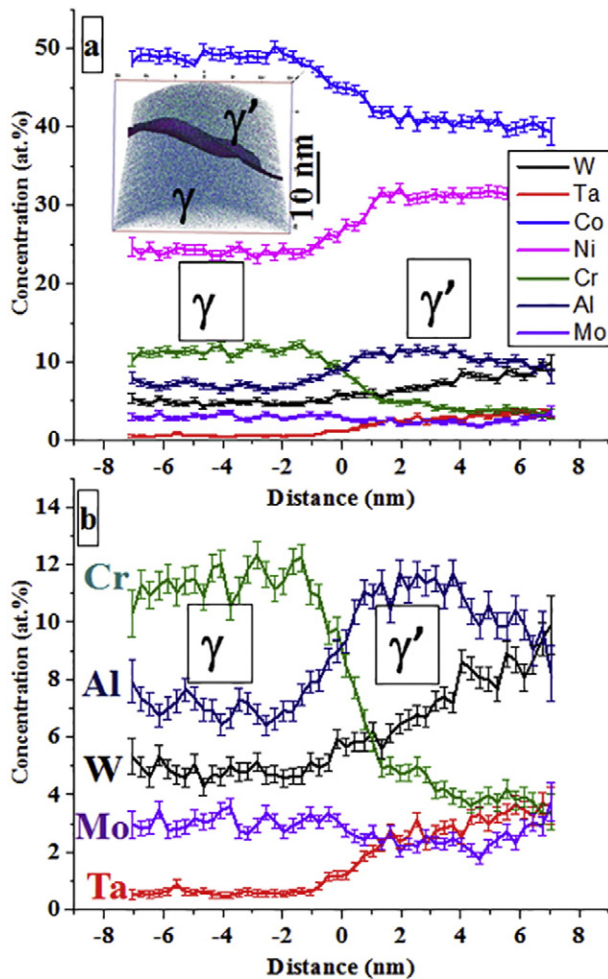


Fig. 3. (a) The proximity histogram showing the solute partitioning across the γ/γ' interface along with the respective APT reconstruction and (b) a magnified section of the proxigram revealing the partitioning of solute atoms in Co–Ni–D.

Co–Ni–B and Co–Ni–D alloys provide further insight to the discussion by Titus et al. and Eggeler et al. [7,8] on the role of chemistry of γ' precipitates on anti-phase boundaries (APB) energies. The APB energy of the γ' phase controls the dislocation shearing mode and contributes to the high temperature creep strength. The APB energies in γ' strengthened Co–Ni–base alloys are lower than those in Co–base and Ni–base superalloys, based on TEM analysis of crept microstructures of two Co–Ni–base alloys, Co–Ni–A and Co–Ni–C, which revealed extensive APBs within γ' precipitates [7,8]. The composition of Co–Ni–A, particularly the Co to Ni ratio, is similar to the alloys being presently studied (Co–Ni–B and Co–Ni–D), which have Co-dominant γ' composition. The Co–Ni–C composition [7] has equal amounts of Co and Ni in atom percent and is quite similar to the V208C alloy investigated by Knop et al. [9]. The atom probe results for V208C are reproduced in Table 1 and clearly indicate a Ni-dominant γ' composition for the γ' precipitates in which 2/3 of the M sites are occupied by Ni. Hence, γ' precipitates in the Co–Ni–A and Co–Ni–C alloys have low APB energies over a large range of Co/Ni ratios based on the γ' phase compositions, further suggesting a dominance of high levels of Co additions to Ni-dominant or large Ni additions to Co-dominant γ' phase in controlling the APB energy within Co–Ni–base alloys. This study indicates that, although the composition and Ni to Co ratio on the M site of the M_3X compound does not solely dictate APB energies, instituting large enough chemistry variations within the extended phase field of Co–Ni–base alloys in order to alter the APB energy significantly enough to change

the γ' deformation mode in Co–Ni alloys may prove challenging. These results raise fundamental questions such as (1) the demarcation between Co and Ni–base superalloys in current Co–Ni–base alloys based on γ' composition and (2) the role of composition of γ' precipitates on APB energy.

Comprehensive APT results of low misfit, multicomponent Co–Ni–base superalloys, in which approximately 1/2 of the Co sites within the $Co_3(Al,W)$ phase are occupied by Ni provide the following insights:

- The partitioning ratio of W reduces to 1 at high Co/Ni ratios relative to simpler quaternary alloys providing the potential for increasing the solid solution strengthening component of the γ phase and enabling a range of lattice misfit, from positive to near-zero.
- The enrichment of W at the $\gamma-\gamma'$ interface is observed in a Co–Ni–base multicomponent alloy that exhibits negligible W partitioning.
- Co–base superalloys with significant additions of Ni can exhibit either Co-dominant or Ni-dominant γ' composition depending on the Co/Ni ratio in the M site of M_3X compound but previous work indicates that the investigated alloys exhibit lower APB energies relative to Co- and Ni-base superalloys. This suggests that, for $\gamma-\gamma'$ alloys with Co/Ni ratios closer to unity, the APB energy is independent of composition.

Acknowledgments

This work has been supported through the Idaho National Laboratory (INL) Laboratory Directed Research & Development (LDRD) Program under DOE Idaho Operations Office Contract DE-AC07-05ID14517. Atom probe tomography and transmission electron microscopy work was carried out at the Center for Advanced Energy Studies-Microscopy and Characterization Suite (CAES-MaCS). TMP additionally acknowledges the support of NSF DMREF Grant # 1233704.

This manuscript has been authored by Battelle Energy Alliance, LLC under Contract No. DE-AC07-05ID14517 with the U.S. Department of Energy. The United States Government retains and the publisher, by accepting the article for publication, acknowledges that the United States Government retains a nonexclusive, paid-up, irrevocable, world-wide license to publish or reproduce the published form of this manuscript, or allow others to do so, for United States Government purposes.

References

- [1] J. Sato, T. Omari, K. Oikawa, I. Ohnuma, R. Kainuma, K. Ishida, *Science* 312 (2006) 90–91.
- [2] A. Suzuki, T.M. Pollock, *Acta Mater.* 56 (2008) 1288–1297.
- [3] A. Bauer, S. Neumeier, F. Pyczak, M. Goken, *Scr. Mater.* 67 (2012) 499–506.
- [4] K. Tannaka, M. Ooshima, N. Tsuno, A. Sato, H. Inui, *Philos. Mag.* 92 (2012) 4011–4027.
- [5] K. Shinagawa, T. Omari, J. Sato, K. Oikawa, I. Ohnuma, R. Kainuma, K. Ishida, *Mater. Trans.* 49 (2008) 1474–1479.
- [6] M.S. Titus, A. Suzuki, T.M. Pollock, *Scr. Mater.* 66 (2012) 574–577.
- [7] Y.M. Eggeler, M.S. Titus, A. Suzuki, T.M. Pollock, *Acta Mater.* 77 (2014) 352–359.
- [8] M.S. Titus, Y.M. Eggeler, A. Suzuki, T.M. Pollock, *Acta Mater.* 82 (2015) 530–539.
- [9] M. Knop, P. Mulvey, F. Ismail, A. Radecka, K.M. Rahman, T.C. Lindley, B.A. Shollock, M.C. Hardy, M.P. Moody, T.L. Martin, P.A.J. Bagot, D. Dye, *JOM* 66 (2014) 2495–2501.
- [10] S.K. Makineni, B. Nithin, K. Chattopadhyay, *Scr. Mater.* 98 (2015) 36–39.
- [11] J.E. Saal, C. Wolverton, *Acta Mater.* 61 (2013) 2330–2338.
- [12] M. Chen, C.Y. Wang, *J. Appl. Phys.* 107 (2010) 093705.
- [13] S.R. Joshi, K.V. Vamsi, S. Kartikeyan, *Mater. Conf. Proc.* 142014 18001.
- [14] M.S. Titus, A. Mottura, G.B. Viswanathan, A. Suzuki, M.J. Mills, T.M. Pollock, *Acta Mater.* (2015) submitted for publication.
- [15] A.R.P. Singh, S. Nag, S. Chattopadhyay, Y. Ren, J. Tiley, G.B. Viswanathan, H.L. Fraser, R. Banerjee, *Acta Mater.* 61 (2013) 280–293.
- [16] M.K. Miller, *Micron* 32 (2001) 757–764.
- [17] D. Blavette, E. Cadel, B. Deconihout, *Mater. Charact.* 44 (2000) 133–157.
- [18] Y. Amouyal, Z. Mao, D.N. Seidman, *Acta Mater.* 58 (2010) 5898–5911.
- [19] S. Meher, S. Nag, J. Tiley, A. Goel, R. Banerjee, *Acta Mater.* 61 (2013) 4266–4276.
- [20] P.J. Bocchini, E.A. Lass, K. Moon, M.E. Williams, C.E. Campbell, U.R. Kattner, D.C. Dunand, D.N. Seidman, *Scr. Mater.* 68 (2013) 563–566.
- [21] S. Meher, R. Banerjee, *Intermetallics* (2014) 138–142.
- [22] S. Meher, H.Y. Yan, S. Nag, D. Dye, R. Banerjee, *Scr. Mater.* 67 (2012) 850–853.

- [23] I. Povstugar, P. Choi, S. Neumeier, A. Bauer, C.H. Zenk, M. Goken, D. Raabe, *Acta Mater.* 78 (2014) 78–85.
- [24] A. Ardell, *Philos. Mag.* 94 (2014) 2101–2130.
- [25] O. Hellman, J.A. Vandenbroucke, J. Rüsing, D. Isheim, D.N. Seidman, *Microsc. Microanal.* 6 (2000) 437–444.
- [26] A. Mottura, A. Janotti, T.M. Pollock, *Intermetallics* 28 (2012) 138–143.
- [27] Y. Amouyal, Z. Mao, D. Seidman, *Appl. Phys. Lett.* 93 (2008) 201905.
- [28] T.M. Pollock, R.D. Field, in: F.R.N. Nabarro, M.S. Duesbery (Eds.), *Dislocations in Solids*, vol. 11, Elsevier, Amsterdam, 2002.